

# Geophysical Research Letters

## RESEARCH LETTER

10.1029/2021GL093661

### Key Points:

- Transition from Gilbert to hyperpycnal delta is a two-stage process involving foundation development and hyperpycnal delta progradation
- The processes during these stages can be quantitatively described by diffusion-based models that reveal strong morphological self-similarity
- Within limited durations the post-transition hyperpycnal deltas approach at higher speed toward the trajectory of the non-transitioned delta

### Supporting Information:

Supporting Information may be found in the online version of this article.

### Correspondence to:

F.-C. Wu,  
fcwu@ntu.edu.tw

### Citation:

Lai, S. Y. J., & Wu, F.-C. (2021). Two-stage transition from Gilbert to hyperpycnal delta in reservoir. *Geophysical Research Letters*, 48, e2021GL093661. <https://doi.org/10.1029/2021GL093661>

Received 2 APR 2021

Accepted 2 JUL 2021

## Two-Stage Transition From Gilbert to Hyperpycnal Delta in Reservoir

Steven Yueh Jen Lai<sup>1</sup>  and Fu-Chun Wu<sup>2</sup> 

<sup>1</sup>Department of Hydraulic and Ocean Engineering, National Cheng Kung University, Tainan, Taiwan, <sup>2</sup>Department of Bioenvironmental Systems Engineering and Hydrotech Research Institute, National Taiwan University, Taipei, Taiwan

**Abstract** Deltas are a most common form of reservoir sedimentation. When the river inflows switch between homopycnal and hyperpycnal, morphological transitions between Gilbert and hyperpycnal deltas take place. So far, however, detailed studies on how such transitions occur and quantitative descriptions of the processes have been rare. Here, we study experimentally the deltaic transitions in response to the switch of flow type. Our results show that transition from hyperpycnal to Gilbert delta is purely depositional. This contrasts the transition from Gilbert to hyperpycnal delta, which is a two-stage process involving both erosion and deposition. During the first stage, hyperpycnal flows modify the existing Gilbert delta into a subaqueous foundation, over which hyperpycnal delta develops and progrades into the basin during the second stage. After transition, hyperpycnal deltas migrate at higher speeds to recover the non-transitioned trajectories. Diffusion-based models are found well suited to describing the self-similar morphodynamics of the two-stage process.

**Plain Language Summary** Reservoirs worldwide have faced declining storage volumes because of sedimentation. Deltas are a most common form of reservoir sedimentation. When the river inflows switched between clear and turbid waters, the morphology of delta experienced a transition between a short, steep slope (called Gilbert delta) and a longer, milder surface (called hyperpycnal delta). Because these two types of delta extend downstream into the reservoir in different styles, and both increase the flood risk at headwater sections, we conducted flume experiments to better understand the transitional processes and the resulting morphologies and behaviors of delta after such transition. Our results reveal that transition from Gilbert to hyperpycnal delta is a two-stage process. During the first stage, a wedge-shaped underwater foundation was developed by eroding the upper part of delta slope and depositing sediment at its lower part. During the second stage, hyperpycnal delta grew on top of the foundation. After transition, hyperpycnal deltas moved at higher speeds to recover their non-transitioned trajectories. The dynamic processes during these two stages can be described by diffusion-based models. These models were used to evaluate the transitional timescales in both laboratory and real-world settings. The results provide novel information on dynamics of reservoir sedimentation.

### 1. Introduction

Lacustrine delta is a most common type of reservoir sedimentation, which forms when a sediment-laden river flow enters a lake or reservoir. The flow may be homopycnal, with identical densities of incoming and receiving waters, or hyperpycnal, with incoming water denser than receiving water. The deltaic morphology associated with homopycnal flows is characterized by a classic Gilbert-type delta, with coarse-grained foreset slope prograding at the angle of repose (Gilbert, 1885). This contrasts the hyperpycnal delta shaped by plunging underflows, which exhibits an elongated, curved foreset of gradually diminishing slope extending toward the dam (Lai & Capart, 2007a, 2009). Examples of Gilbert-type delta in reservoir have been documented in the side tributary of Wushe Reservoir (central Taiwan), Englebright Lake of northern California, and Lake Mills of western Washington State (Ke & Capart, 2015; Snyder et al., 2006; Stratton & Grant, 2019). Well-known hyperpycnal deltas in reservoir have been exemplified by the Colorado River delta in Lake Mead, Tarbela delta in the upper Indus River (northern Pakistan), and rapid infill of Wushe Reservoir by the trunk river delta (Ke et al., 2019; Kostic et al., 2002; Lai & Capart, 2009; Lai, et al., 2019).

Transitions between different types of delta have been reported in reservoirs that experienced shifts in sediment regime, flow type, or density contrast. In Taiwan, for instance, a transition from hyperpycnal to

Gilbert-type delta has been documented in the small Ronghua Reservoir (Lai & Capart, 2009), where river inflow was highly turbid during flood and a hyperpycnal delta was initially developed. This hyperpycnal delta then transformed into a Gilbert delta because the small reservoir swiftly became turbid itself, diminishing the density contrast between inflow and lake. In the laboratory, a transition from Gilbert to hyperpycnal delta was observed as the inflow switched from homopycnal (clear water fed with coarse sediment) to hyperpycnal (turbid water fed with coarse sediment) (Kostic et al., 2002). A transition from hyperpycnal to Gilbert delta has been documented in small-scale hyperpycnal flow experiments (brine fed with coarse sediment) where the basin was ultimately ponded with brine, reducing the density contrast between inflow and lake (Lai & Capart, 2007a).

Given the highly probable shifts in flow/sediment regimes and in relative density that could be triggered by natural or anthropic disturbances (Lai et al., 2019; Stratton & Grant, 2019), we need a better understanding of the corresponding morphological responses to forecast the spatial distribution of deltaic deposits in reservoirs. So far, however, no dedicated study has been conducted to investigate how such transitions occur and whether these processes can be quantitatively described. In this experimental study, we restrict our attention to the deltaic transitions in response to a switch between homopycnal and hyperpycnal flows while keeping both the liquid and sediment supply rates constant, and static basins of constant water levels. We seek to answer three research questions. (a) What is the fundamental difference between the transition from Gilbert delta to hyperpycnal delta and that from hyperpycnal to Gilbert delta? (b) Can the transitional processes be described by quantitative models? (c) Can the post-transition delta recover the morphodynamics of the pure (non-transitioned) Gilbert or hyperpycnal delta?

## 2. Experiments

### 2.1. Experimental Setting

Experiments were conducted in a small flume (270 cm long, 1 cm wide) installed in an external water tank, modified from Lai et al. (2019), Lai, Hsiao and Wu (2017) (see Figure S1 for details). Constant inflows per unit width ( $Q = 263.2 \pm 9.3 \text{ mm}^2/\text{s}$ ) of clear water and saturated brine (density  $\rho_{\text{in}} = 1,200 \text{ kg/m}^3$ ) were used, respectively, as homopycnal and hyperpycnal flows (Lai et al., 2016, 2019, Lai, Hung, et al., 2017), fed with constant sand influxes per unit width ( $I = 15.4 \pm 0.3 \text{ mm}^2/\text{s}$ ), with  $Q/I = 17.2 \pm 0.9$  that established supply limited conditions (Lai et al., 2019). Ottawa standard sand (with median grain size  $d_{50} = 0.17 \text{ mm}$ , density  $\rho_s = 2670 \text{ kg/m}^3$ , porosity  $n_0 = 0.51$ , angle of repose  $\phi = 36^\circ$ ) was used as bedload material for deltaic deposits. Effects of capillary and cohesive forces were not significant in our experiments (Text S1). Time-lapse photography was used to record morphological evolutions, with images acquired every 5 s. The deltaic profiles were then extracted by image digitization and coordinate conversion.

Three series of experiments (Series 13.5, 10, and 6.5) were conducted with the bed slope angle  $\theta = 13.5^\circ$ ,  $10^\circ$ , and  $6.5^\circ$ , respectively, typical values for bedrock rivers in mountain areas (Lai et al., 2019). Each series includes four runs with the run names ending by G, H, PG, and PH (Table S1). For the first two runs (G, H), the flow type switched every 900 s to create periodic transitional processes. The name ending by G indicates a run starting with Gilbert delta (i.e., homopycnal flow); the name ending by H indicates a run starting with hyperpycnal delta (i.e., hyperpycnal flow). In Series 13.5 and 10, each run lasted for 5,400 s (6 cycles); in Series 6.5, however, each run lasted only for 3,600 s (4 cycles) since the head of the topset (bedrock-alluvial transition) had reached the upstream end of the flume. The last two runs (PG and PH), were performed with pure Gilbert and hyperpycnal deltas without switching the flow type. These two serve as the reference runs.

### 2.2. Experimental Observations

Transitions from Gilbert to hyperpycnal delta and from hyperpycnal to Gilbert delta exhibited two distinct morphodynamic processes (see Movies S1–S6). Under constant inflow of clear water, Gilbert delta prograded steadily into the basin (Figure 1a). Upon the switch to hyperpycnal flow, a two-stage transition from Gilbert to hyperpycnal delta was observed. During Stage 1, the hyperpycnal flow eroded the nearshore upper foreset and deposited sediment at the foreset toe (Figure 1b). A wedge-shaped subaqueous platform, termed “foundation” herein, quickly developed. Progressive erosion of the upper foreset during Stage 1 led to the

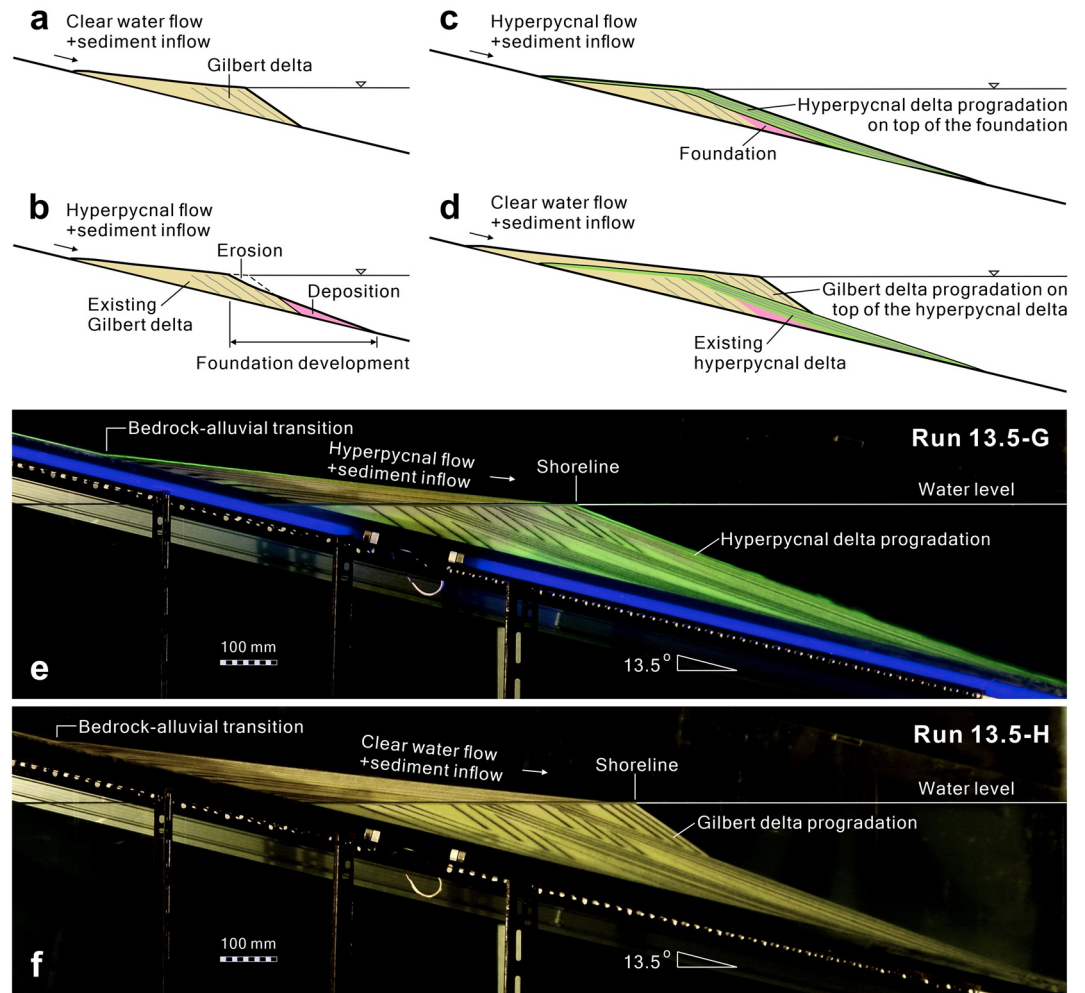


**Figure 1.** Transitions between Gilbert and hyperpycnal deltas: (a) Gilbert delta progradation with inflows of clear water and sand; (b) Stage 1: erosion of upper foreset by hyperpycnal flow and deposition at the foreset toe of Gilbert delta, forming a wedge-shaped foundation; (c) Stage 2: hyperpycnal delta progradation over the foundation; (d) Gilbert delta progradation over the hyperpycnal delta after switch to homopycnal flow. Deltaic morphologies and stratigraphic structures at the end of (e) Run 13.5-G, and (f) Run 13.5-H.

retreat of shoreline (topset-foreset slope break). The speed of shoreline retreat declined quickly to zero, then the transitional process entered Stage 2. During this stage, a well-defined hyperpycnal delta prograded on top of the foundation (Figure 1c), resuming the advance of shoreline.

By contrast, transition from hyperpycnal to Gilbert delta was purely depositional (Figure 1d). Gilbert delta developed directly over the topset and upper foreset face of the existing hyperpycnal delta without involving erosional processes. The resulting morphology was hybrid, with Gilbert delta prograding over the elongated foreset bed of hyperpycnal delta. The noncovered part of the foreset bed will serve as the basement for foundation development during subsequent transitions. Shown in Figures 1e and 1f are deltaic morphologies at the end of Runs 13.5-G and 13.5-H, where the coal ashes highlight the distinct stratigraphic structures of Gilbert and hyperpycnal deltas. The foreset of hyperpycnal delta is characterized by elongated, concave, and thin layers of deposits, while the foreset of Gilbert delta is characterized by steep, straight, and thick layers of deposits held at the angle of repose. The topset layers of hyperpycnal delta are thinner than those of Gilbert delta because hyperpycnal underflows transport more sediment further downstream.

The above-stated transitional processes apply to all slope angles used and all experiments either starting with Gilbert or hyperpycnal delta (see Figures S2 and S3 for full demonstration of six transitional runs). Because transition from hyperpycnal to Gilbert delta is a simple depositional process over the topset and

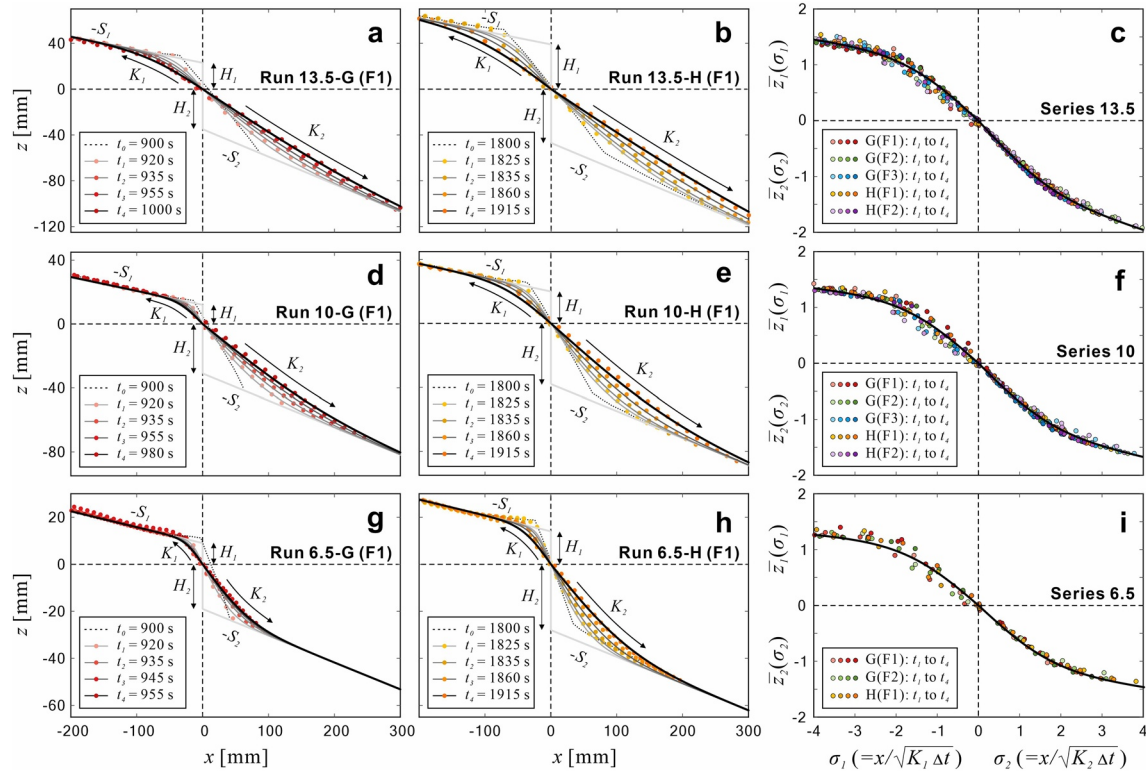


**Figure 2.** Series 13.5, 10, and 6.5: (a–b, d–e, g–h) Experimental and theoretical profiles (color symbols and solid lines) during the first cycles of foundation development; (c, f, and i) normalized profiles during different cycles of foundation development, where  $\Delta t = t - t_0$  is the length of time since starting time  $t_0$ .

foreset of hyperpycnal delta, such transition is not substantially different from Gilbert delta progradation over two-slope bedrock presented in earlier studies (Lai et al., 2017a, 2019). Thus, when answering the second research question posed in Section 1, we focus on quantitative descriptions of the two-stage transitional processes from Gilbert to hyperpycnal delta.

### 2.3. Deltaic Long Profiles

To track the morphological evolutions, in each cycle of transition (900 s) we extracted four long profiles (at  $t = T_1$  to  $T_4$ , with equal intervals of 200 s) from the time-lapse images. Besides, within each cycle of foundation development, we extracted four long profiles (at  $t = t_1$  to  $t_4$ , with selected intervals) by carefully reviewing the time-lapse images to demarcate the time  $t_4$  when foundation development completed, that is, when shoreline retreat changed to shoreline advance (see Table S2 for a summary of these times). Foundation development was a quick process, the length of time ( $t_4 - t_0$ ) taken to complete the process ranged from 55 to 220 s, increasing with the starting time  $t_0$  of the cycle (Figure S4). As stated in Section 2.1, for experiments starting with Gilbert delta, three cycles of foundation development, denoted as G(F1), G(F2), and G(F3), were observed in Series 13.5 and 10, and two cycles, G(F1) and G(F2), were observed in Series 6.5; whereas for experiments starting with hyperpycnal delta, two cycles of foundation development, H(F1) and H(F2), were observed in Series 13.5 and 10, and one cycle H(F1) was observed in Series 6.5.

## 3. Results

### 3.1. Two-Stage Transition From Gilbert to Hyperpycnal Delta

Shown in Figure 2a, 2b, 2d, 2e, 2g and 2h are deltaic profiles extracted from the first cycles of foundation development under different initial settings, G(F1) and H(F1), in Series 13.5, 10, and 6.5. Evolutions of

deltaic profile  $z(x, t)$  exhibit simultaneous landward erosion and basinward deposition, resembling the knickpoint migration process described by a diffusion model (Hanks et al., 1984; Mitchell, 2006):

$$z(x, t) = -H \cdot \operatorname{erf}\left(\frac{x}{2\sqrt{Kt}}\right) - Sx \quad (1)$$

where  $H$  = knickpoint height (shape factor);  $\operatorname{erf}$  = error function (shape function);  $K$  = diffusivity;  $S$  = far-field slope. The first and second terms on the right-hand side of Equation 1 account for the variations of bed profile caused by the geomorphic diffusion and initial bed slope, respectively. These figures also show asymmetric profiles of landward erosion and basinward deposition, suggesting that different parameters,  $(H_1, K_1, S_1)$  and  $(H_2, K_2, S_2)$ , be used for the upstream and downstream bed profiles (Table S1). The values of these parameters increase with the bed slope angle  $\theta$  (Figure S5), indicating stronger effects of geomorphic diffusion and initial bed slope associated with greater  $\theta$ .

To investigate the self-similarity of the evolving profiles in various settings, the first and second terms on the right-hand side of Equation 1 are, respectively, normalized by the shape factor  $H$  and the time-varying length scale  $\sqrt{Kt}$ . As a result, the normalized profile  $\bar{z}$  is time-invariant, varying only as a function of the dimensionless horizontal coordinate  $\sigma (= x / \sqrt{Kt})$  (Capart et al., 2007):

$$\bar{z}(\sigma) = -\operatorname{erf}\left(\frac{\sigma}{2}\right) - S\sigma \quad (2)$$

The normalized profiles during different cycles of foundation development are shown in Figures 2c, 2f and 2i for Series 13.5, 10, and 6.5, where the upstream and downstream profiles,  $\bar{z}_1$  and  $\bar{z}_2$ , are plotted against the dimensionless coordinates  $\sigma_1$  and  $\sigma_2$ , respectively. The experimental profiles at different times ( $t_1$  to  $t_4$ ) for different cycles (F1, F2, F3) in different settings (G and H) collapse on single theoretical curves depicted by Equation 2, indicating that the evolving profiles during Stage 1 (foundation development) share strong, inherent self-similarity.

As mentioned earlier, the growth of hyperpycnal delta over a well-developed foundation during Stage 2 is purely depositional, which can be described by a two-diffusion model of hyperpycnal delta progradation (Lai & Capart, 2009; Lai et al., 2019). This model describes the joint geomorphic actions of subaerial and subaqueous flows as two diffusion processes with different strengths and transport thresholds, and treats the bedrock-alluvial transition and topset-foreset transition as two moving boundaries. It yields self-similar analytical solutions for the co-evolving topset and foreset bed profiles (see Text S2 for details). To validate this model, we compared the experimental profiles of hyperpycnal delta at  $t = T_1$  to  $T_4$  with the theoretical profiles for different cycles of Stage 2 (H1, H2, and H3) in different initial settings (G and H). Good agreement between the experimental and theoretical profiles is evident (Figure S6). We further examined the self-similarity of the evolving profiles in various settings by comparing the normalized profiles  $z / \sqrt{Kt}$  versus  $x / \sqrt{Kt}$  (Figure S7). Collapse of experimental profiles on single theoretical profiles confirmed that the morphological evolutions during Stage 2 were governed by the self-similar, two-diffusion process of hyperpycnal delta progradation.

### 3.2. Completion Time of Foundation Development

So far, we have known that Stage 1 (foundation development) is described by a diffusion model of knickpoint migration, Stage 2 (delta growth) is described by a two-diffusion model of hyperpycnal delta progradation. This raises a question concerning the completion time of foundation development: when will Stage 1 be completed and enter Stage 2? Here we hypothesize that foundation development is completed when the profile developed during Stage 1 reaches an appearance that is closest to the profile of hyperpycnal delta developed during Stage 2. Specifically, the completion time  $t_c$  can be defined as the time when the morphological difference between the foundation and hyperpycnal delta reaches a minimum. To test this hypothesis, we used these two models to calculate the profiles of foundation and hyperpycnal delta over a range of time and identified the time  $t_c$  that corresponded to the minimum absolute difference. An example is given in Figures 3a and 3b for the first cycle in Run 13.5-G, where the identified  $t_c = 1,060$  s, and the foundation and

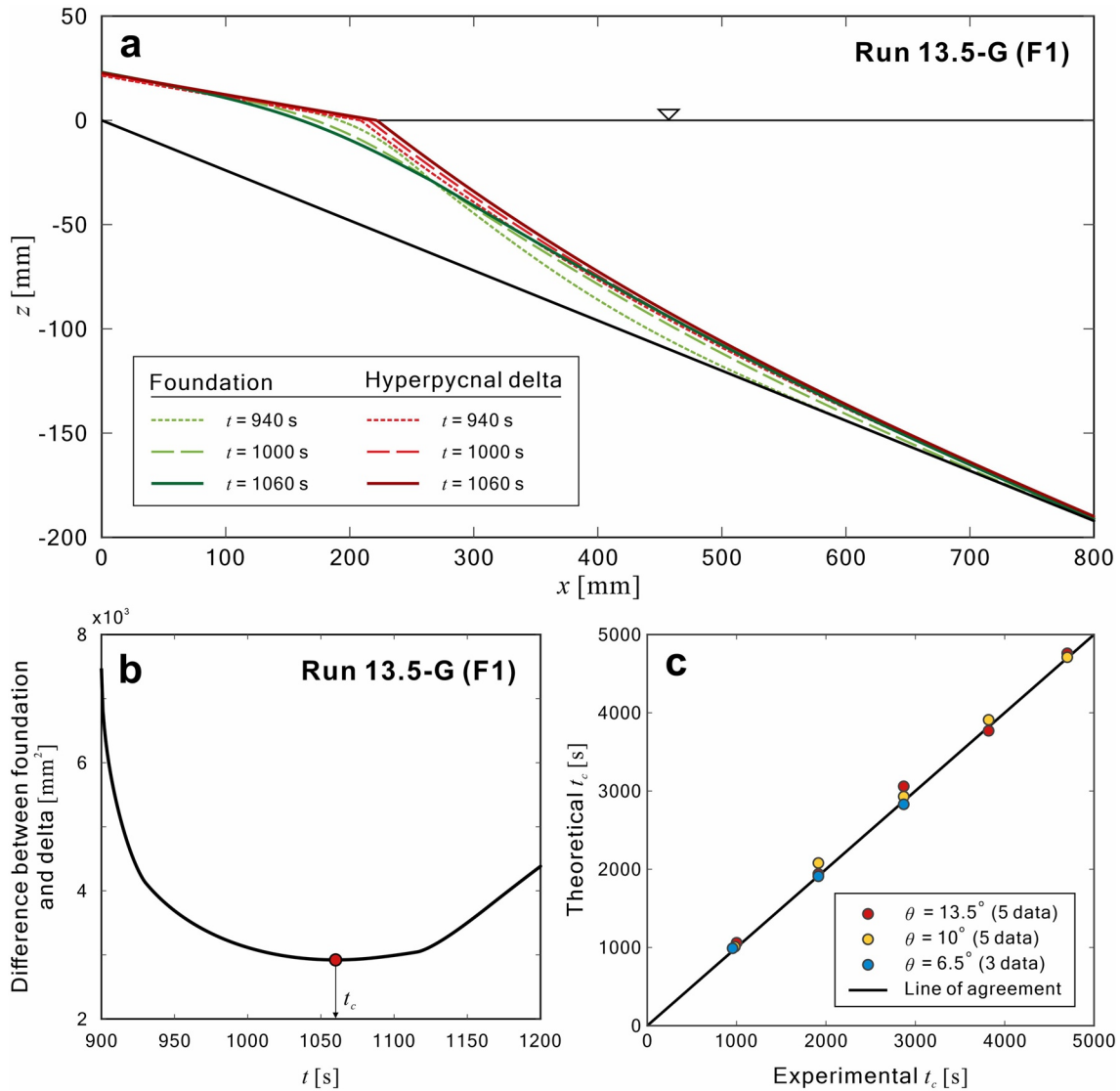


**Figure 3.** (a–b) An example illustrating determination of completion time  $t_c$ , and profiles of foundation and hyperpycnal delta at three different times during the first cycle of transition in Run 13.5-G; (c) agreement plot between theoretical and experimental  $t_c$  for 13 cycles of transition observed in this study.

delta profiles at  $t = 940, 1,000,$  and  $1,060$  s are shown to demonstrate that the two profiles reach an optimal match at  $1,060$  s. For all 13 cycles of transition observed, the values of  $t_c$  so determined are compared with those demarcated from the time-lapse images, with excellent agreement shown in Figure 3c (see Figure S8 for a full demonstration of the results).

### 3.3. Recovery of Pure Gilbert and Hyperpycnal Deltas

To explore whether the post-transition delta can recover the morphodynamics of the pure (non-transitioned) delta, we tracked the trajectory of depocenter (centroid) during each cycle of transition, as shown in Figure 4, where the cycles of Gilbert and hyperpycnal delta progradation, and foundation development are labeled as (G1, G2, G3), (H1, H2, H3), and (F1, F2, F3), respectively. The envelope curves are the trajectories of depocenter of the pure Gilbert and hyperpycnal deltas extracted from the six reference runs (PG and PH). The depocenter of the pure hyperpycnal delta advanced faster than that of the corresponding pure Gilbert delta, primarily attributable to the much longer foreset shaped by hyperpycnal underflows. A unique trait of Series 6.5, where the depocenter of the pure Gilbert delta retreated rather than advanced, was attributed

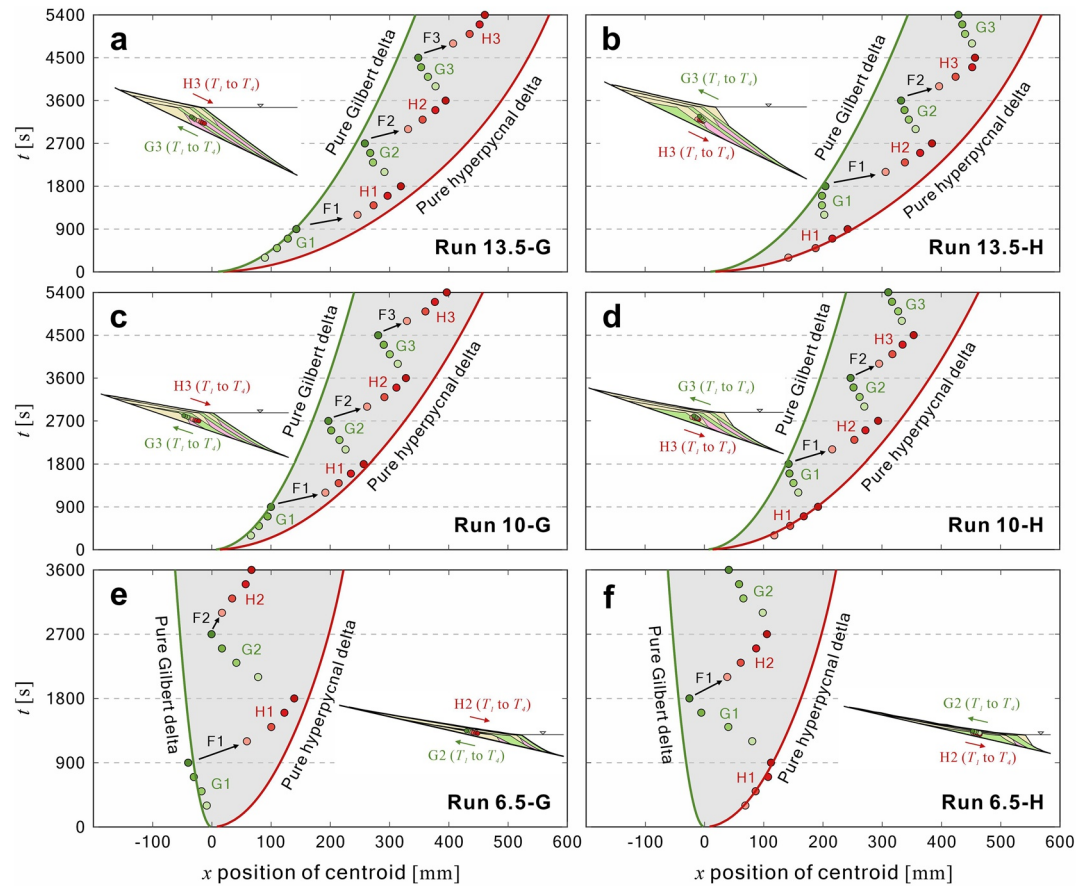


**Figure 4.** Trajectory of depocenter during each cycle of transition in (a–b) Series 13.5; (c–d) Series 10; (e–f) Series 6.5. Cycles of Gilbert delta and hyperpycnal delta progradation, and foundation development are denoted as (G1, G2, G3), (H1, H2, H3), and (F1, F2, F3). Color symbols denote  $T_1$  to  $T_4$  of each cycle.

to the development of a longer, thicker topset over the mildest bed slope used (see raw images uploaded to Zenodo repository).

During each cycle the post-transition delta tend to recover the morphodynamics of the pure delta by migration of depocenter at higher speeds  $dx / dt$  toward the envelope curve (1.1–3.2 times the corresponding speeds in the pure deltas). Within the limited duration of each cycle (900 s), however, none of the post-transition deltas ever recovered the trajectory of the pure delta. The end-of-cycle discrepancy in depocenter between the pure and post-transition deltas increased with time, due to the opposite migrations of depocenter in the post-transition hyperpycnal and Gilbert deltas, the former basinward whereas the latter landward. Such opposite migrations arose from the fact that foreset is the major part of growth in the post-transition hyperpycnal delta whereas topset is the major part of growth in the post-transition Gilbert delta (Figures 1c and 1d). The opposite growth styles rendered the recovery of pure deltas increasingly difficult with the progressing cycle of transition.

#### 4. Discussion

In this section we provide answers to the research questions posed, discuss their implications for interpreting the transitional behaviors of the deltaic deposits, and present a real-world application of the two-stage transition model.

#### 4.1. Fundamental Difference in Deltaic Transitions

Our results reveal a fundamental difference in the transitions between Gilbert and hyperpycnal deltas. Transition from hyperpycnal to Gilbert delta in response to a switch from hyperpycnal to homopycnal flow is purely depositional, characterized by direct progradation of Gilbert delta over the upper foreset of existing hyperpycnal delta. By contrast, transition from Gilbert to hyperpycnal delta in response to a switch from homopycnal to hyperpycnal flow is a two-stage process involving both erosion and deposition. Hyperpycnal flows exhibit a strong capability to modify the morphology of preexisting Gilbert delta into a subaqueous foundation (Stage 1), over which hyperpycnal delta progrades steadily into the basin (Stage 2). A very similar morphological transition involving both erosional and depositional processes has been documented by Kostic et al. (2002). They observed in laboratory erosion of the upper foreset and a slide deposit that formed at the lower foreset face of Gilbert delta, following a switch from homopycnal to hyperpycnal inflow. The slide deposit was subsequently buried by the prograding hyperpycnal delta. A related, but not exactly matched, field case is the initial phase of delta degradation in response to partial drawdown flushing of Lake Mills during the removal of Glines Canyon Dam on the Elwha River (Washington, USA) (Randle et al., 2015). In this case reservoir drawdown increments of 3–5 m gave rise to 20 m of incision through the topset, which resulted in 2–10 m of deposition on top of prodelta and lakebed deposits. This incision of topset contrasts the upper-foreset erosion caused by a shift in flow type from homopycnal to hyperpycnal.

The basal shear stresses applied by the hyperpycnal flows act to augment gravity, thus reducing the slope needed for sediment transport. The observed erosion of the upper foreset and deposition at the foreset toe by hyperpycnal flows is a process of slope readjustment (Ross et al., 1994; Gerber et al., 2008). Such type of foreset erosion has been previously hypothesized as a potential mechanism for incision of nearshore submarine canyons during base-level rise, and ravinement of shoreface deposits during transgression (Lai & Capart, 2007b; Paola et al., 2009). Our results demonstrate that a shift from homopycnal to hyperpycnal flow alone can initiate erosion of the deltaic foresets, without the need of the base-level rise or transgression. If the hyperpycnal flows persist, however, the readjusted foreset slope would act as a subaqueous foundation favorable for hyperpycnal delta progradation and would be eventually overlaid by the prograding delta. The stratigraphic records would exhibit only partial Gilbert deltas with their upper foresets eroded, accompanied by the foundation deposits that extend downstream of the foreset fronts. These are important findings with broad applicability to stratigraphic interpretation.

#### 4.2. Quantitative Descriptions of Two-Stage Transition

The two-stage transition from Gilbert to hyperpycnal delta can be described by two quantitative models. Stage 1 (foundation development) is described by a diffusion model of knickpoint migration, with different parameter values (diffusivity, shape factor, and far-field slope) used for the landward erosion and basinward deposition. The diffusivity  $K_2$  for the basinward deposition is 7–14 times ( $\sim O(10)$  greater than) the corresponding value of  $K_1$  for the landward erosion; the shape factor  $H_2$  and far-field slope  $S_2$  are both twice ( $O(1)$  greater than) the corresponding values of  $H_1$  and  $S_1$ . The stronger basinward deposition than the landward erosion suggests that these deposits source from both the eroded material and the upstream sediment supply, transported by the highly competent hyperpycnal underflows. The parameter values depend also on the morphological relief of the preexisting Gilbert delta, thus increasing with the bed slope angle. The normalized experimental profiles at different times for different cycles in different settings collapse on single theoretical curves, confirming that the evolving foundation profiles, despite asymmetric, exhibit strong morphological self-similarity.

During Stage 2, the evolution of delta over a well-developed subaqueous foundation is a purely depositional process described by a two-diffusion model of hyperpycnal delta progradation. Collapse of the normalized experimental profiles on single theoretical profiles also confirms the self-similarity of such process. Using the two-stage transition model, the completion time  $t_c$  of Stage 1 is defined as the time when the evolving foundation profile optimally matches the profile of hyperpycnal delta that develops during Stage 2, or when the morphological self-similarity of hyperpycnal delta resumes. Good agreement between the theoretical and experimental  $t_c$  indicates that foundation development paves the way for the stage of hyperpycnal delta progradation. The time taken to complete foundation development increases with the progressing cycle of transition due to the associated greater relief of the preexisting Gilbert delta.

To further examine the morphodynamics of foundation at  $t = t_c$ , we evaluate sediment flux  $j$  at location  $s$  using the theoretical profile of foundation  $z(x, t_c)$  (Lai & Capart, 2009; Lai et al., 2019):

$$j(s, t_c) = I + \frac{[z(s, t_c) - z_0(s)]s}{2t_c} - \frac{1}{t_c} \int_{-\infty}^s [z(x, t_c) - z_0(x)] dx \quad (3)$$

where  $z_0$  = initial bed profile. Once the sediment flux along the bed is reconstructed, the bed growth rate  $\partial z / \partial t$  can be evaluated with the gradient of sediment flux according to the continuity equation of sediment:

$$\partial z / \partial t = -\partial j / \partial x \quad (4)$$

The results (see Figures S8–1 to S8–13) reveal that the bed growth rate peaks in the nearshore region where the discrepancy between the optimally matched profiles of foundation and hyperpycnal delta is maximum, indicating that at  $t = t_c$  the fastest growth of bed elevation in the nearshore region works to eliminate such discrepancy within a shortest time, moving the transitional process to Stage 2.

#### 4.3. Recovery of Non-Transitioned Pure Delta

Under identical flow and sediment supply conditions, the advance of depocenter in the non-transitioned pure hyperpycnal delta is faster than the migration of depocenter in the pure Gilbert delta, the latter would even retreat given a mild enough bed slope. The trajectories of depocenter in the pure hyperpycnal and Gilbert deltas constitute the front and rear envelope curves in  $t$ - $x$  plane. The trajectories of depocenter in the post-transition deltas are bounded by these envelope curves. For a transition from Gilbert to hyperpycnal delta, the depocenter migrates downstream to the front envelope curve; for a transition from hyperpycnal to Gilbert delta, the depocenter migrates upstream to the rear envelope curve. Within limited durations, the depocenters of the post-transition deltas can only approach the envelope curves. Given long enough durations, however, the post-transition deltas may be able to recover the morphodynamics of the pure deltas because the migration speeds of the depocenters,  $dx / dt$ , in the post-transition deltas are on average 2.1 times the corresponding speeds in the non-transitioned pure deltas (Figure 4).

#### 4.4. Application of Two-Stage Transition Model to Po Delta (Italy)

To demonstrate the utility of the two-stage transition model in a real-world setting, we evaluate the time taken to complete foundation development in the Po delta (Tolle lobe) located at the Adriatic coast of Italy. This site was selected because a detailed reconstruction of the evolving deltaic profile during the past 300 years is available from combined cartographic data with seismic-stratigraphic and core data (Correggiari et al., 2005). Tolle prodelta lobe has been the dominant distributary of the Po delta since the end of the Little Ice Age. Climatic change, anthropogenic causes (deforestation and artificial levees) or breaching of natural dams during this period led to catastrophic increases in water discharge and sediment load that generated hyperpycnal flows. As a result, Tolle lobe advanced as a hyperpycnal delta between 1736 and 1811 (Figure 5a). From 1811 to 1860, in response to a decline in fine-sediment supply caused by human impacts (damming, river excavation, and land reclamation), Tolle lobe underwent a morphological transition, then advanced as a Gilbert delta from 1860 to 1880. Since 1886, short-lived episodes of increased discharge and sediment load (of natural or artificial origin) again generated hyperpycnal flows, Tolle lobe underwent a retreat associated with subaqueous channel formation through a cut-and-fill process, similar to that of foundation development. By 2002, the retreat of Tolle lobe has come to a halt, resuming the progradation of hyperpycnal delta. Although it is not a lacustrine delta, Tolle lobe exhibited a deltaic evolution resembling the two-stage transition process presented in this work, and provides an excellent opportunity for scaling up the experimental finding into a real-world setting.

To apply the two-stage transition model to the Tolle lobe, the parameters must first be calibrated with the evolving deltaic profiles (Figures 5b and 5c). The foundation profiles of 1886, 1905 and 1932 were used to determine the parameters of Stage 1 (foundation development); the hyperpycnal delta profiles of 1736, 1811 and 2002 were used for those of Stage 2 (hyperpycnal delta progradation). The parameter values are

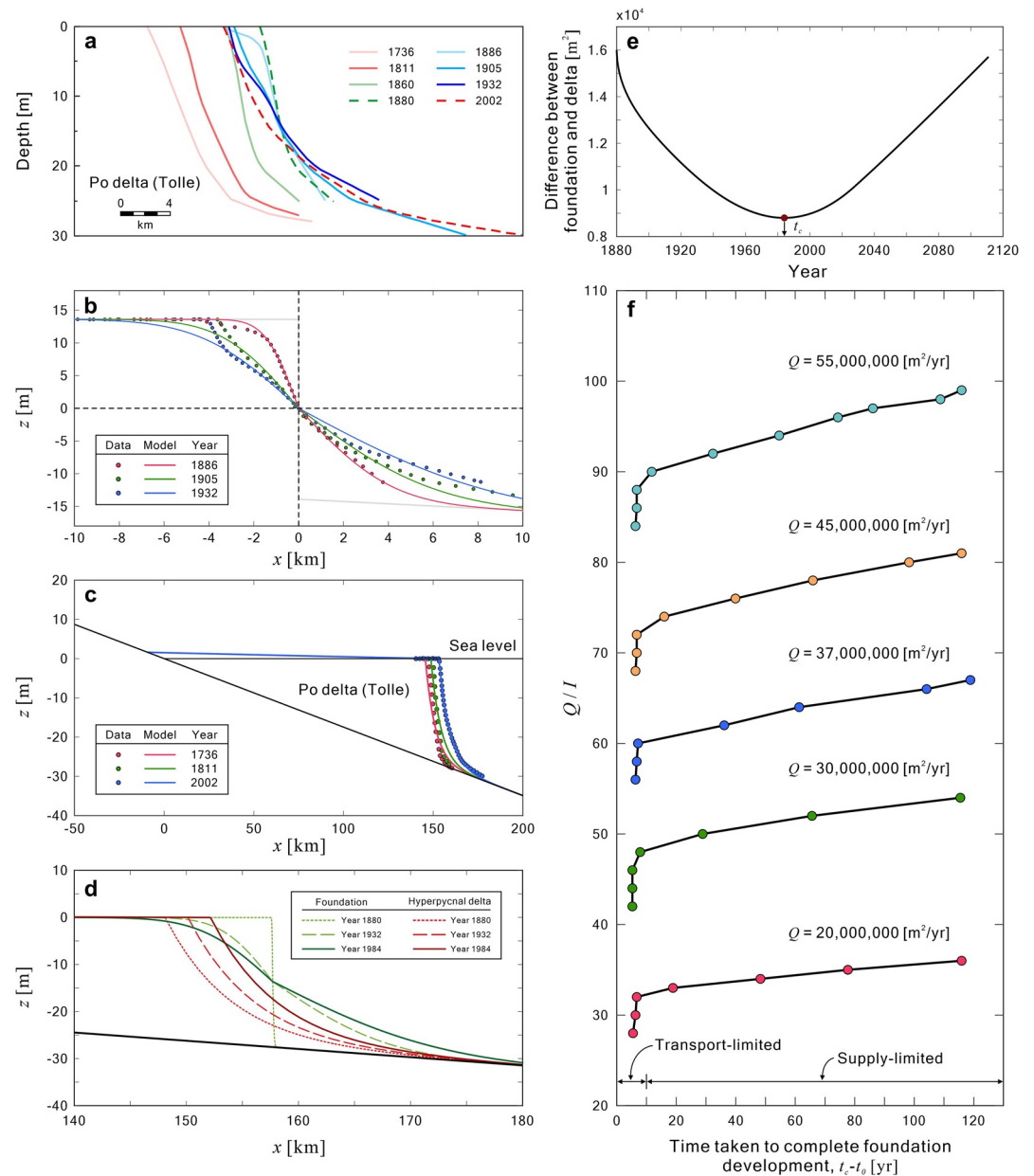


**Figure 5.** (a) Reconstructed subaqueous profiles of Po delta (Tolle lobe) during 1736–2002 (redrawn from Correggiari et al. (2005)). Parameters calibration with evolving profiles of Po delta: (b) foundation profiles (1886, 1905, 1932), and (c) hyperpycnal delta profiles (1736, 1811, 2002). Calculated evolution of Po delta since 1880: (d) profiles of foundation and hyperpycnal delta; (e) temporal variation of the profile difference between foundation and hyperpycnal delta. (f) Phase diagram of  $t_c - t_0$ , time taken to complete foundation development, as a function of  $Q$  and  $Q / I$ , for Po delta.

summarized in Table S3, where the mean annual discharge of Tolle lobe during 1918–2003 (when hyperpycnal flows prevailed) and mean width of 154 m (Correggiari et al., 2005; Syvitski et al., 2005) were used to estimate the unit-width discharge  $Q = 37 \text{ M m}^2/\text{yr}$ . The calibrated  $Q / I = 66$  is reasonable, slightly greater than the value  $Q / I = 40$  that corresponds to an upper-bound estimate of  $I = 925 \text{ K m}^2/\text{yr}$  required for generating hyperpycnal flows, based on the mean annual sediment load (1918–1987) (Correggiari et al., 2005). The density of inflow used,  $\rho_{\text{in}} = 1,040 \text{ kg/m}^3$ , corresponds to a suspended-sediment concentration of 64 g/L, which exceeds the threshold of 40 g/L required for generating hyperpycnal flows in marine environments, where the average ambient ocean density is  $1,025 \text{ kg/m}^3$  (Mulder & Syvitski, 1995; Warrick & Milliman, 2003).

To evaluate the time taken to complete foundation development in Tolle lobe, the initial time  $t_0$  was set to be 1880, when the last profile of Gilbert delta prior to the retreat in 1886 is available. The evolving profiles of foundation and hyperpycnal delta and temporal variation of their difference (see Figures 5d and 5e) show that the completion time  $t_c$  corresponding to the minimum difference is 1984. The time taken to complete foundation development,  $t_c - t_0$ , is thus 104 years, in concordance with the observation that progradation of hyperpycnal delta resumed before 2002, that is,  $t_c - t_0 < 122$  years. The reason for such a long time taken to complete Stage 1 in Tolle lobe, which contrasts the quick process observed in our experiments, is that hyperpycnal flow events are highly pulsed, commonly occur during brief periods (hours to occasionally days), totaling about 0.1%–0.2% of the total time (Warrick and Milliman, 2003). The result thus indicates that, with robust parameter calibration, even a simple diffusion-based model can reproduce the two-stage transition process of Tolle lobe and scale up the timescale of such process into a real-world setting.

With the parameters of Tolle lobe, a phase diagram of  $t_c - t_0$  as a function of  $Q / I$  is provided (Figure 5f) for a realistic range of  $Q$  (20–55 M m<sup>2</sup>/yr). The phase diagram reveals three traits that deserve mention. First, for a specific  $t_c - t_0$  (>10 years), the corresponding  $Q / I$  values on different curves are proportional to the  $Q$  value of each curve while the associated  $I$  values remain identical. This indicates that  $t_c - t_0$  is determined by  $I$  rather than  $Q$ , which arises from the supply limited condition established when sediment supply rate  $I$  is less than the sediment transport capacity of  $Q$ . Second, for a given  $Q$ , the value of  $t_c - t_0$  increases with  $Q / I$  because of the associated decrease in  $I$  for the reason stated above. Third, for a given  $Q$ , the increase in  $t_c - t_0$  per unit decrease of  $I$ ,  $-d(t_c - t_0) / dI$ , increases with declining  $I$ , indicating that  $t_c - t_0$  varies more sensitively with the variation of smaller  $I$  rather than larger  $I$ . For example, for those data points on the left end of each curve, where  $I$  values are all >615 K m<sup>2</sup>/yr, the corresponding values of  $t_c - t_0$  (<10 years) differ by very limited amounts. This suggests that, while  $I$  is a dominating control on  $t_c - t_0$ , it no longer has significant effects on  $t_c - t_0$  when sediment supply rate  $I$  exceeds the transport capacity of  $Q$ .

The results highlight the effects of hyperpycnal flow discharge  $Q$  and sediment supply rate  $I$  on the transitional timescale. The effect of  $Q$  on such timescale is indirect, mainly through determination of sediment transport capacity. When  $I$  is less than the transport capacity of  $Q$  (i.e., supply limited conditions), the time required for foundation development decreases with the increase of  $I$ . When  $I$  is greater than the transport capacity of  $Q$  (i.e., transport-limited conditions), the time required for foundation development no longer decreases with the increase of  $I$  because sediment transport rate is limited by  $Q$ . These conditions should be distinguished when applying the model and phase diagram.

## Data Availability Statement

A full data set is available at: <https://zenodo.org/record/4620332#.YFQlt68zaUk>.

## Acknowledgments

Funding of this study was granted by the Ministry of Science and Technology (MOST), Taiwan, to Fu-Chun Wu (107-2221-E-002-029-MY3, 109-2221-E-002-012-MY3) and Steven Yueh Jen Lai (108-2119-M-006-007, 109-2628-E-006-006-MY3). Tai-Lin Ou is acknowledged for carrying out the experiments. We are grateful to two anonymous reviewers for constructive comments that helped improve the paper.

## References

- Capart, H., Bellal, M., & Young, D. L. (2007). Self-similar evolution of semi-infinite alluvial channels with moving boundaries. *Journal of Sedimentary Research*, 77, 13–22. <https://doi.org/10.2110/jsr.2007.009>
- Correggiari, A., Cattaneo, A., & Trincardi, F. (2005). The modern Po Delta system: Lobe switching and asymmetric prodelta growth. *Marine Geology*, 222–223, 49–74. <https://doi.org/10.1016/j.margeo.2005.06.039>
- Gerber, T. P., Pratson, L. F., Wolinsky, M. A., Steel, R., Mohr, J., Swenson, J. B., & Paola, C. (2008). Cliniform progradation by turbidity currents: Modeling and experiments. *Journal of Sedimentary Research*, 78, 220–238. <https://doi.org/10.2110/jsr.2008.023>
- Gilbert, G. K. (1885). The topographic features of lake shores. *Annu. Rep. USGS*, 5, 69–123.
- Hanks, T. C., Bucknam, R. C., Lajoie, K. R., & Wallace, R. E. (1984). Modification of wave-cut and faulting-controlled landforms. *Journal of Geophysical Research*, 89, 5771–5790. <https://doi.org/10.1029/jb089ib07p05771>
- Ke, W.-T., & Capart, H. (2015). Theory for the curvature dependence of delta front progradation. *Geophysical Research Letters*, 42(10), 10680–10688. <https://doi.org/10.1002/2015GL066455>
- Ke, W.-T., Wang, W.-L., Liu, H.-H., Chang, J.-Y., Huang, Y.-C., & Capart, H. (2019). Rapid infill of Wushe Reservoir, Central Taiwan: Ten years of field observations. *Proceedings of the 3rd International Workshop on Sediment Bypass Tunnels*, National Taiwan University, Taipei, Taiwan.
- Kostic, S., Parker, G., & Marr, J. G. (2002). Role of turbidity currents in setting the foreset slope of cliniforms prograding into standing fresh water. *Journal of Sedimentary Research*, 72, 353–362. <https://doi.org/10.1306/081501720353>
- Lai, S. Y. J., & Capart, H. (2007a). Two-diffusion description of hyperpycnal deltas. *Journal of Geophysical Research*, 112, F03005. <https://doi.org/10.1029/2006JF000617>
- Lai, S. Y. J., & Capart, H. (2007b). Response of hyperpycnal deltas to a steady rise in base level. In C. M. Dohmen-Janssen, & S. J. M. H. Hulscher (Eds.), *Proceedings of the 5th IAHR symposium on river, coastal and estuarine morphodynamics* (pp. 57–62). CRC Press. <https://doi.org/10.1201/noe0415453639-c8>

- Lai, S. Y. J., & Capart, H. (2009). Reservoir infill by hyperpycnal deltas over bedrock. *Geophysical Research Letters*, *36*, L08402. <https://doi.org/10.1029/2008GL037139>
- Lai, S. Y. J., Chiu, Y. -J., & Wu, F. -C. (2019). Self-similar morphodynamics of Gilbert and hyperpycnal deltas over segmented two-slope bedrock channels. *Water Resources Research*, *55*, 3689–3707. <https://doi.org/10.1029/2018WR023824>
- Lai, S. Y. J., Gerber, T. P., & Amblas, D. (2016). An experimental approach to submarine canyon evolution. *Geophysical Research Letters*, *43*, 2741–2747. <https://doi.org/10.1002/2015GL067376>
- Lai, S. Y. J., Hsiao, Y.-T., & Wu, F.-C. (2017). Asymmetric effects of subaerial and subaqueous basement slopes on self-similar morphology of prograding deltas. *Journal of Geophysical Research: Earth Surface*, *122*, 2506–2526. <https://doi.org/10.1002/2017JF004244>
- Lai, S. Y. J., Hung, S. S. C., Foreman, B. Z., Limaye, A. B., Grimaud, J.-L., & Paola, C. (2017). Stream power controls the braiding intensity of submarine channels similarly to rivers. *Geophysical Research Letters*, *44*, 5062–5070. <https://doi.org/10.1002/2017GL072964>
- Mitchell, N. C. (2006). Morphologies of knickpoints in submarine canyons. *GSA Bulletin*, *118*, 589–605. <https://doi.org/10.1130/B25772.1>
- Mulder, T., & Syvitski, J. P. M. (1995). Turbidity currents generated at river mouths during exceptional discharges to the world oceans. *The Journal of Geology*, *103*, 285–299. <https://doi.org/10.1086/629747>
- Paola, C., Straub, K., Mohrig, D., & Reinhardt, L. (2009). The “unreasonable effectiveness” of stratigraphic and geomorphic experiments. *Earth-Science Reviews*, *97*, 1–43. <https://doi.org/10.1016/j.earscirev.2009.05.003>
- Randle, T. J., Bountry, J. A., Ritchie, A., & Wille, K. (2015). Large-scale dam removal on the Elwha River, Washington, USA: Erosion of reservoir sediment. *Geomorphology*, *246*, 709–728. <https://doi.org/10.1016/j.geomorph.2014.12.045>
- Ross, W. C., Halliwell, B. A., May, J. A., Watts, D. E., & Syvitski, J. P. M. (1994). Slope readjustment: A new model for the development of submarine fans and aprons. *Geology*, *22*, 511–514. [https://doi.org/10.1130/0091-7613\(1994\)022<0511:sranmf>2.3.co;2](https://doi.org/10.1130/0091-7613(1994)022<0511:sranmf>2.3.co;2)
- Snyder, N. P., Wright, S. A., Alpers, C. N., Flint, L. E., Holmes, C. W., & Rubin, D. M. (2006). Reconstructing depositional processes and history from reservoir stratigraphy: Englebright Lake, Yuba River, northern California. *Journal of Geophysical Research*, *111*, F04003. <https://doi.org/10.1029/2005JF000451>
- Stratton, L. E., & Grant, G. E. (2019). Autopsy of a reservoir: Facies architecture in a multidam system, Elwha River, Washington, USA. *GSA Bulletin*, *131*, 1794–1822. <https://doi.org/10.1130/b31959.1>
- Syvitski, J. P. M., Kettner, A. J., Correggiari, A., & Nelson, B. W. (2005). Distributary channels and their impact on sediment dispersal. *Marine Geology*, *222–223*, 75–94. <https://doi.org/10.1016/j.margeo.2005.06.030>
- Warrick, J. A., & Milliman, J. D. (2003). Hyperpycnal sediment discharge from semiarid southern California rivers: Implications for coastal sediment budgets. *Geology*, *31*, 781–784. <https://doi.org/10.1130/g19671.1>

## References From the Supporting Information

- Lick, W., Jin, L., & Gailani, J. (2004). Initiation of movement of quartz particles. *Journal of Hydraulic Engineering*, *130*, 755–761.
- Malverti, L., Lajeunesse, E., & Métivier, F. (2008). Small is beautiful: Upscaling from microscale laminar to natural turbulent rivers. *Journal of Geophysical Research*, *113*, F04004. <https://doi.org/10.1029/2007JF000974>